

# Gum Arabic-Coated Magnetic Nanoparticles For Methylene Blue Removal

Eman Alzahrani

Assistant Professor, Department of Chemistry, Faculty of Science, Taif University, 888-Taif, Kingdom of Saudi Arabia

**ABSTRACT:** Magnetic nanoparticles (MNPs) were fabricated using the chemical co-precipitation method followed by coating the surface of magnetic  $\text{Fe}_3\text{O}_4$  nanoparticles with gum arabic (GA). The fabricated magnetic nanoparticles were characterised using transmission electron microscopy (TEM) which showed that the  $\text{Fe}_3\text{O}_4$  nanoparticles and GA-MNPs nanoparticles had a mean diameter of 33 nm, and 38 nm, respectively. Scanning electron microscopy (SEM) images showed that the MNPs modified with GA had homogeneous structure and agglomerated. The energy dispersive X-ray spectroscopy (EDAX) spectrum showed strong peaks of Fe and O. X-ray diffraction patterns (XRD) indicated that the naked magnetic nanoparticles were pure  $\text{Fe}_3\text{O}_4$  with a spinel structure and the covering of GA did not result in a phase change. The covering of GA on the magnetic nanoparticles was also studied by BET analysis, and Fourier transform infrared spectroscopy. Moreover, the present study reports a fast and simple method for removal and recovery of methylene blue dye (MB) from aqueous solutions by using the synthesised magnetic nanoparticles modified with gum arabic as adsorbent. The experimental results show that the adsorption process attains equilibrium within five minutes. The data fit the Langmuir isotherm equation and the maximum adsorption capacities were  $8.77 \text{ mg mg}^{-1}$  and  $14.3 \text{ mg mg}^{-1}$  for MNPs and GA-MNPs, respectively. The results indicated that the homemade magnetic nanoparticles were quite efficient for removing MB and will be a promising adsorbent for the removal of harmful dyes from waste-water.

**KEYWORDS:**  $\text{Fe}_3\text{O}_4$  magnetic nanoparticles; Gum arabic; Co-precipitation; Adsorption dye; Methylene blue; Adsorption isotherm.

## I. INTRODUCTION

Recently, environmental problems have attracted greater attention all over the world. One of the environmental pollutants is synthetic dye, commonly used for colouring materials such as textiles, leather, paper, wool, printed matter, and cosmetics [1]. Many of these dyes are toxic and carcinogenic to human beings; therefore, several researchers are working on methods for the removal of dyes from waste-water before discharging into downstream bodies of water [2].

Magnetic nanoparticles (MNPs) that possess a magnetite ( $\text{Fe}_3\text{O}_4$ ) or maghemite ( $\gamma\text{-Fe}_2\text{O}_3$ ) core chemistry have been used to solve environmental problems; for example, MNPs have been utilised for purification of waste-water by removing heavy metals, alkalinity and hardness, natural organic compounds and salt[3]. This is because of simple fabrication, easy optimisation of their size and morphology, and fast magnetic separation under an external magnetic field [4].

Iron oxide nanoparticles can be fabricated using different methods; for example, co-precipitation [5], energy milling [6], reducing [7], and ultrasonic assisted impregnation [8]. The co-precipitation method is based on mixing ferrous and ferric ions at the ratio of 1 to 2 in an alkaline medium. The main advantage of this method is that it produces fine and stoichiometric particles of single and multi-component metal oxides [9]. In order to improve their physicochemical properties and to achieve different kinds of applications, modification of the surface of magnetic nanoparticles with functional groups is necessary [4].

# International Journal of Innovative Research in Science, Engineering and Technology

(An ISO 3297: 2007 Certified Organization)

Vol. 3, Issue 8, August 2014

Gum arabic (*Acacia Senegal species*), Figure 1, is a natural exudate obtained from the stem or branches of *Acacia senegal* and *Acacia seyal* trees of the Sahel region of Africa [10]. It is a widely used ingredient in the food and pharmaceutical industries; for example it is found in dairy products, beverages, confectionery and gummy candies, textiles, paints, ink, liquid adhesives, pharmaceutical and cosmetic products [11, 12]. GA is a negatively charged, hydrophilic non-toxic branched complex polysaccharide existing as mixed calcium, magnesium, and potassium salts [13]. The protein in GA is rich in hydroxypropyl, prolyl and seryl residues covalently linked to carbohydrate moieties [14]. Many groups have utilised GA in drug delivery systems [15], carriers for the micro-encapsulation of bioactive molecules [16], and in the field of nanotechnology [17]. This is because of its biocompatibility and its stabilisation of nanostructure.

The main objective of this study was to synthesise iron oxide magnetic nanoparticles by co-precipitation methods, followed by modification of the surface of the fabricated nanoparticles with GA. The structure morphology of the fabricated materials was characterised using BET analysis, transmission electron microscopy (TEM), scanning electron microscopy-energy dispersive X-ray spectroscopy (SEM-EDAX), X-ray diffraction (XRD), and Fourier transform infrared spectrometer (FT-IR). Methylene blue dye (MB) removal by naked magnetic nanoparticles and magnetic nanoparticles modified with GA was assessed.



Fig. 1 Image of gum arabic.

## II. MATERIAL AND METHODS

### A. Chemicals, Materials, and Instrumentation

Ammonium hydroxide solution (25%), iron (II) chloride tetrahydrate ( $\text{FeCl}_2 \cdot 4\text{H}_2\text{O}$ ), iron (III) chloride hexahydrate ( $\text{FeCl}_3 \cdot 6\text{H}_2\text{O}$ ), and commercial methylene blue ( $\text{C}_{16}\text{H}_{18}\text{N}_2\text{Na}_2\text{O}_6\text{S}_3$ ) textile dye (99%) was purchased from Sigma-Aldrich (Nottingham, UK) and used without further purification. Gum arabic (GA) was purchased from a local supermarket in Taif, KSA. Cylindrical rod magnets (40 mm diameter x 40 mm thick) for settlement of magnetic nanoparticles was purchased from Magnet Expert Ltd. (Tuxford, UK). Distilled water was employed for preparing all the solutions and reagents.

A hot plate stirrer from VWR International LLC (West Chester, PA, USA) was used. The Brunauer-Emmett-Teller (BET) model used a Surface Area and Porosity Analyser from Micromeritics Ltd. (Dunstable, UK). The transmission electron microscopy (TEM) came from JEOL Ltd. (Welwyn Garden City, UK). The scanning electron microscope - energy dispersive X-ray spectroscopy (SEM-EDAX) Cambridge S360 came from Cambridge Instruments (Cambridge, UK). The UV-Vis spectrophotometer came from Thermo Scientific™ GENESYS 10S (Toronto, Canada). The X-ray

# International Journal of Innovative Research in Science, Engineering and Technology

(An ISO 3297: 2007 Certified Organization)

Vol. 3, Issue 8, August 2014

diffraction (XRD) came from Rigaku Ltd. (Ettlingen, Germany). A WiseTherm high temperature muffle furnace came from Wisd Laboratory Instrument (Wertheim, Germany). The FT-IR spectra were collected in the attenuated total reflectance (ATR) mode using a PerkinElmer RX FTIR  $\times 2$  with diamond ATR, DRIFT attachment from PerkinElmer (Buckinghamshire, UK).

## **B. Synthesis of $Fe_3O_4$ Nanoparticles and Surface Modification of MNPs with GA**

Fabrication of magnetic nanoparticles was performed by co-precipitation of ferric ions ( $Fe^{3+}$ ) and ferrous ions ( $Fe^{2+}$ ) in presence of ammonium hydroxide solution (25%). This was performed by dissolving 4.58 g of  $FeCl_2 \cdot 4H_2O$  and 8.93 g  $FeCl_3 \cdot 6H_2O$  in 80 mL distilled water. The mixture was heated to  $80^\circ C$  with vigorous stirring (1,100 rpm). Then, 10 mL of ammonium hydroxide ( $NH_4OH$ ) solution was added to the mixture. In order to ensure complete growth of nanoparticle crystals, the reaction was allowed to continue for 30 minutes under the same conditions. After that the resulting suspension was cooled down to room temperature and washed with distilled water several times. Finally, the magnetic nanoparticles were isolated using an external magnetic field and dried in an oven at  $50^\circ C$ .

The surface of the  $Fe_3O_4$  nanoparticles was coated with gum arabic by mixing 0.5 g of nanoparticles with 50 mL of GA solution ( $5\text{ mg L}^{-1}$ ). Then, the mixture was sonicated for 30 minutes at room temperature. The gum arabic coated magnetic nanoparticles that formed were recovered from the reaction solution by placing a magnet under the bottle, followed by washing the magnetic nanoparticles with distilled water several times. Finally, they were dried in an oven at  $40^\circ C$  for 24 hours before use.

## **C. Characterisation of the Fabricated Materials**

Both bare MNPs and MNPs modified with gum arabic (GA-MNPs) were studied for their structures. The BET parameters (surface area and average diameter) of MNPs and GA-MNPs were performed by measuring  $N_2$  isotherms at 77 K. All samples were outgassed at 400 K under vacuum for 6 hours. The morphology and mean size of the samples were determined by transmission electron microscopy (TEM). A drop of well-dispersed nanoparticle dispersion was placed onto the amorphous carbon-coated 200 mesh copper grid and allowed to dry at ambient temperature, then the grid was scanned. The morphology of the fabricated magnetic nanoparticles before and after modification with GA was characterised by SEM analysis. The compositional analysis was performed using energy dispersive analysis of X-ray spectroscopy (EDAX). Phase identification and structural analysis of the magnetic nanoparticles were carried out using X-ray diffraction (XRD) with the Cu K $\alpha$  radiation ( $\lambda = 1.5405\text{ \AA}$ ) in the 2-theta range from  $20^\circ$  to  $70^\circ$ . Fourier transform infrared spectroscopy (FT-IR) of MNPs and GA-MNPs were collected in the range  $4000\text{--}400\text{ cm}^{-1}$ , six scans with a resolution of  $4\text{ cm}^{-1}$  were taken to confirm the presence of GA on the surface of the magnetic nanoparticles.

## **D. Separation Process**

The removal of methylene blue dye from an aqueous solution by MNPs and GA-MNPs as adsorbent was investigated by mixing 25 mg of fabricated nanoparticles with 50 mL of methylene blue ( $40\text{ mg L}^{-1}$ ) in a test tube. Then the tube was placed into hot plate stirrer, and the mixture was stirred at 350 rpm for varying lengths of contact time (5 min, 10 min, 15 min, 20 min, 25 min, 30 min, 35 min, 40 min, 45 min, 50 min, 55 min, and 60 min) at room temperature and this test was repeated three times. Then the magnetic nanoparticles were separated from the solution by magnet for 30 seconds. Percent removed and adsorbed amount of the dye was measured using spectrophotometry of the dye before and after the test at maximum wavelength ( $\lambda = 668\text{ nm}$ ) and computing concentration from the calibration curve. The effect of temperature on adsorption of dye was studied using different temperatures (300 K, 310 K, 320 K, and 330 K). Kinetics of adsorption was studied by analysing adsorptive uptake of the dye colour from the aqueous solution at different time intervals.

The percentage of dye removal was calculated using the following equation:

$$\text{Percentage removal of MB (\%)} = \frac{C_o - C_e}{C_o} \times 100 [18]$$

Where  $C_o$  and  $C_e$  are the initial and equilibrium liquid phase concentration of methylene blue, respectively ( $\text{mg L}^{-1}$ )

# International Journal of Innovative Research in Science, Engineering and Technology

(An ISO 3297: 2007 Certified Organization)

Vol. 3, Issue 8, August 2014

The amount of adsorption of dye onto the magnetic nanoparticles was calculated using the following equation:

$$q_e = \frac{C_o - C_e}{W} \times V [18]$$

Where  $q_e$  is the adsorption capacity ( $\text{mg g}^{-1}$ ),  $W$  is the weight of the dry adsorbent used (g), and  $V$  is the volume of dye solution (L).

### III. EXPERIMENTAL RESULTS

#### A. Fabrication of Magnetic Nanoparticles

Magnetic nanoparticles play an important role in many areas of chemistry, physics, and material science [6, 19]. The aim of this study was to investigate the use of magnetic nanoparticles coated with gum arabic as an adsorbent for methylene blue dye. In this study, MNPs were fabricated by co-precipitation of  $\text{Fe}^{2+}$  and  $\text{Fe}^{3+}$  salts from aqueous solution by the addition of a base, which was ammonium hydroxide solution. The fabricated magnetic nanoparticles have supermagnetic properties making them very susceptible to magnetic fields and they can be separated easily from the solution. Figure 2 shows that the fabricated magnetic nanoparticles were separated in 30 seconds after applying an external magnetic field indicating a fast separation process for the microspheres.

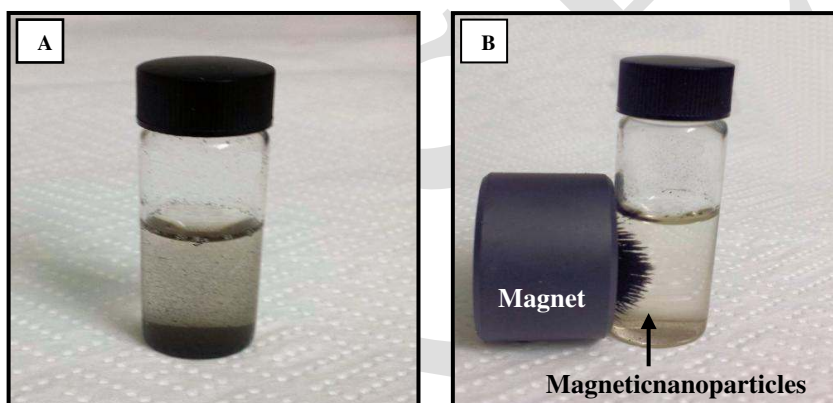


Fig.2 Visual image of magnetic nanoparticles (A), and after separation the magnetic nanoparticles to the sidewall of the sample vial using an external magnet (B).

The structure of the fabricated nanoparticles was studied using TEM analysis, as can be seen in Figure 3 (A), which shows that the magnetic nanoparticles fabricated in this study were multi-dispersed with an average diameter of 33 nm. Figure 3 (B) shows the SEM micrographs of the naked  $\text{Fe}_3\text{O}_4$  nanoparticles, which show that the fabricated material had a homogeneous structure and are in the nano range. In addition, the SEM micrographs showed that MNPs had different shapes that were separated from each other. The particle clusters were observed due to the magnetic interaction between the particles and agglomeration of crystallite occurred to some extent during preparation of the sample.



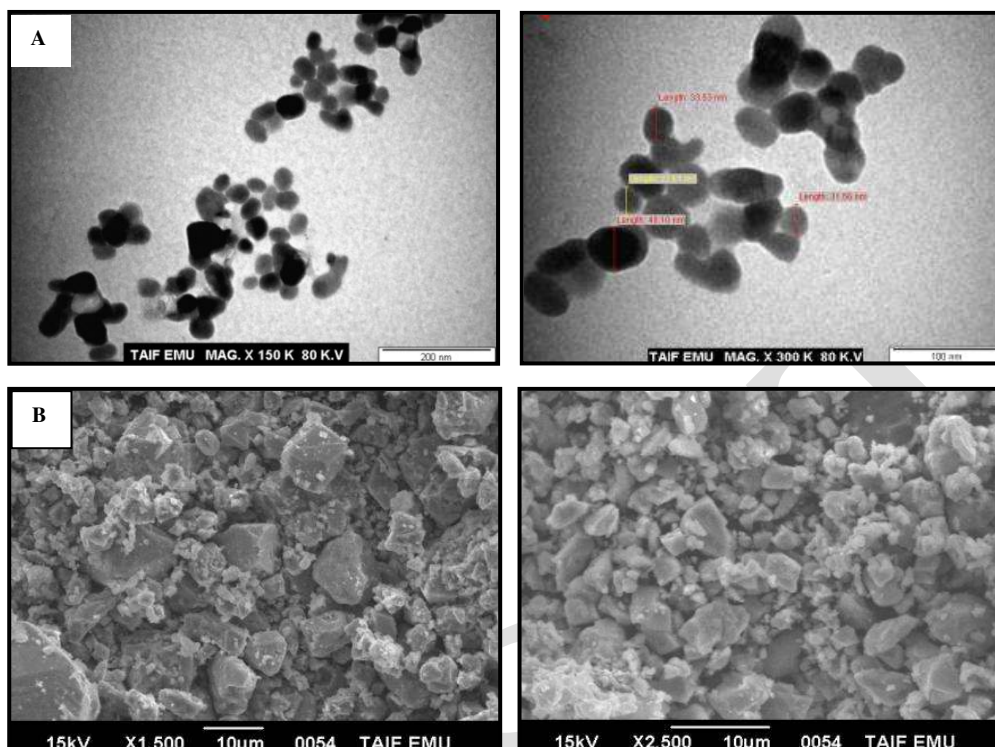


Fig. 3 TEM images (A) and SEM images (B) of bare Fe<sub>3</sub>O<sub>4</sub> nanoparticles.

**B. Modification the Surface of MNP with GA**

In this study, the surface of Fe<sub>3</sub>O<sub>4</sub> nanoparticles was coated with GA in order to improve the selectivity of the magnetic nanoparticles for removing cationic dye. GA and Fe<sub>3</sub>O<sub>4</sub> aqueous slurry were mixed to form GA-MNPs. During preparation, some agglomeration of particles was observed. The fabricated materials were characterised through different techniques such as BET analysis, TEM analysis, SEM analysis, EDAX analysis, XRD analysis, and FT-IR spectroscopy. From the BET analysis it was found that the BET surface area and pore volume of the magnetic nanoparticles were 9.05 m<sup>2</sup> g<sup>-1</sup> and 0.048 cm<sup>3</sup> g<sup>-1</sup> respectively, with an average diameter of 330.6 Å. After coating the MNPs with GA, it was found that the BET surface area, pore volume, and mean diameter were increased to 12.36 m<sup>2</sup> g<sup>-1</sup>, 0.115 cm<sup>3</sup> g<sup>-1</sup>, and 365.8 Å, respectively. The BET parameters are summarised in Table 1. These results confirmed the immobilisation of GA on the surface of naked MNPs.

Table 1 The BET parameters of MNPs and GA-MNPs.

Sample	Surface area (m <sup>2</sup> g <sup>-1</sup> )	Pore volume (cm <sup>3</sup> g <sup>-1</sup> )	Mean diameter (Å)
MNPs	9.05	0.048	330.6
GA-MNPs	12.36	0.115	365.8

The change in the surface of magnetic nanoparticles after coating with GA was investigated using TEM analysis. Figure 4 (A) shows TEM micrographs of Fe<sub>3</sub>O<sub>4</sub> nanoparticles coated with GA. From the figure, it was found that the overall mean diameter of magnetic particles was slightly increased after modification of the surface of MNPs with GA (roughly 38 nm) compared with the mean diameter of unmodified magnetic nanoparticles. This is due to the agglomeration of MNPs which might be due to the high molecular weight of GA [20]. In addition, the morphology and size details were studied by the SEM measurement, as can be seen in Figure 4 (B). The SEM micrograph of GA-MNPs showed they have a homogeneous structure and are agglomerated. It is clear from the SEM micrographs the diameter size of the isolated GA-MNPs was increased.

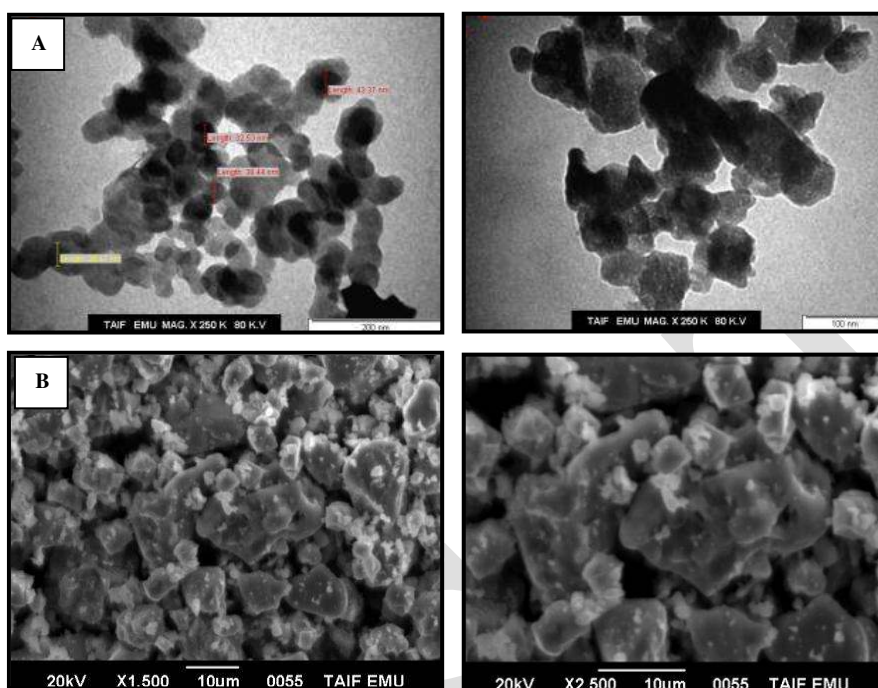


Fig. 4 TEM images (A), and SEM micrographs (B) of Fe<sub>3</sub>O<sub>4</sub> nanoparticles modified with GA.

Besides SEM and TEM analysis, the magnetic nanoparticles were characterised using energy dispersive X-ray (EDAX) analysis in order to identify the elemental components of a sample. Figure 5 shows the EDAX spectrum of GA-MNP, which shows that different compositions were recorded. The result shows strong peaks for Fe and O. This spectrum reveals the composition components of Fe<sub>3</sub>O<sub>4</sub> by co-precipitation synthesis: Fe was 75.87%, and O was 22.25%. GA is composed of organic materials which should be detected as carbon in the EDAX instrument; however, the signal of carbon was not detected in the EDAX spectrum.

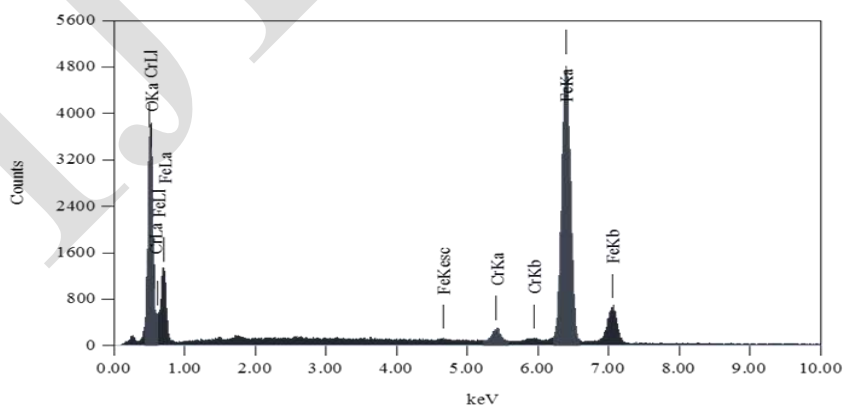


Fig. 5 Energy dispersive analysis of X-ray spectrum (EDAX) of GA-MNPs sample.

## International Journal of Innovative Research in Science, Engineering and Technology

(An ISO 3297: 2007 Certified Organization)

Vol. 3, Issue 8, August 2014

The X-ray diffraction (XRD) patterns of the fabricated magnetic nanoparticles were studied, as can be seen in Figure 6. The analysis of the diffraction pattern shows peaks of the  $\text{Fe}_3\text{O}_4$  nanoparticles at  $2\theta = 30^\circ, 35^\circ, 43^\circ, 53^\circ, 57^\circ, 62^\circ$  which were corresponding to the (220), (311), (400), (422), (511), and (440) crystal planes of a pure  $\text{Fe}_3\text{O}_4$  with spinel structure [19]. From the X-ray diffraction result of GA-MNPs, it was found that modification of the surface of MNPs with GA did not change the spinel structure of MNPs because of the presence of all the XRD peaks mentioned above in the XRD pattern of GA-MNPs.

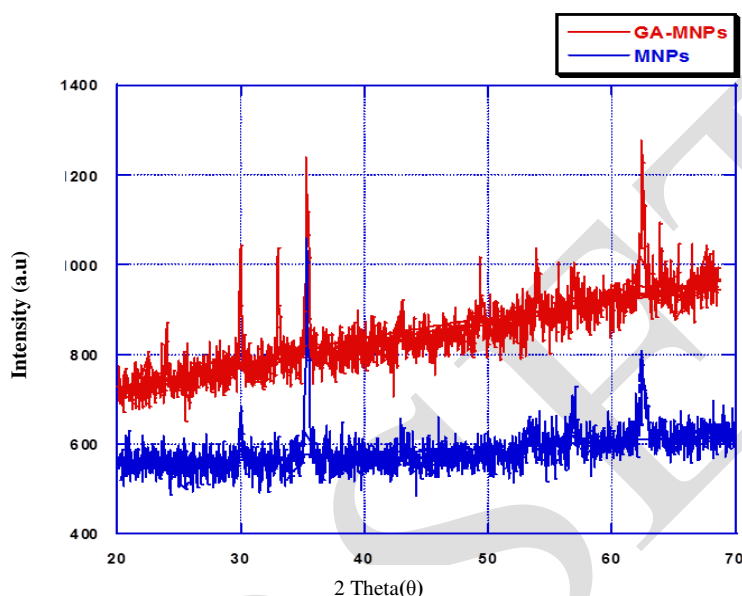


Fig.6 Powder X-ray diffraction pattern of  $\text{Fe}_3\text{O}_4$  (blue line), and  $\text{Fe}_3\text{O}_4$  after modification with GA (red line).

Figure 7 presents the infrared spectra of MNPs, GA-MNPs, and gum arabic. In the MNP spectrum, Figure 7 (A), the strong absorption bands at  $559\text{ cm}^{-1}$  correspond to Fe-O vibration confirm the spinel type structure of pure  $\text{Fe}_3\text{O}_4$ [21]. In addition, the FT-IR of naked MNPs also shows two small broad absorption bands appearing at  $2324\text{ cm}^{-1}$  and  $2101\text{ cm}^{-1}$ , which is attributed to the  $\text{CO}_2$  vibration [22]. In the FT-IR spectrum of gum arabic, Figure 7 (C), the characterisation IR feature indicates the presence of the absorption bands that appear at  $988, 1036,$  and  $1067\text{ cm}^{-1}$  which are attributed to C-O stretching vibration, while the absorption band at  $1641\text{ cm}^{-1}$  is due to the C=O stretching vibration. The absorption band at  $1453\text{ cm}^{-1}$  is due to the C-O stretching vibration. The absorption bands that appear at  $2869\text{ cm}^{-1}$  and  $2941\text{ cm}^{-1}$  may be attributed to C-H stretching. In addition, the abroad absorption band at  $3000\text{ cm}^{-1}$  and  $3600\text{ cm}^{-1}$  which is the characteristic peak of -OH groups stretch of the polysaccharide. In Figure 7 (B), it was found that after modification with gum arabic, the characteristic absorption bands attributed to gum arabic were observed in FT-IR spectrum of GA-MNPs. Therefore the conclusion can be drawn that GA was successfully coated the magnetic nanoparticles.

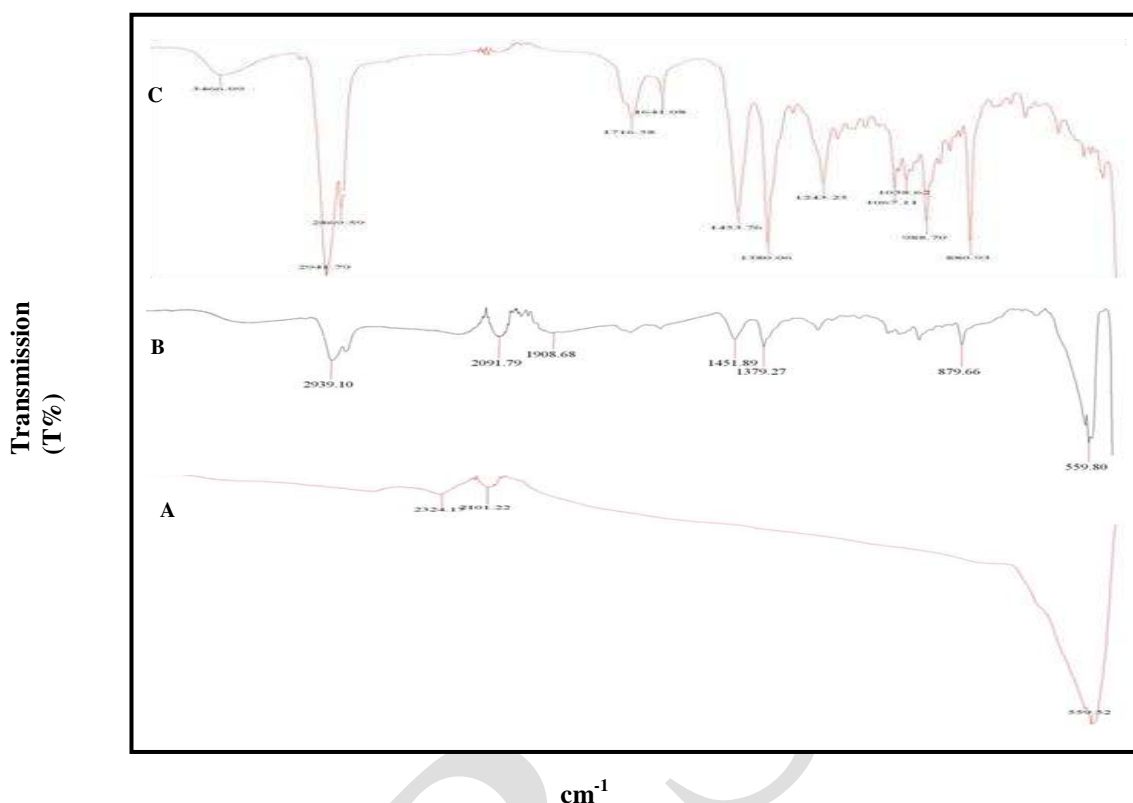


Fig.7 The infrared spectra of (A) naked magnetic nanoparticles, (B) gum arabic immobilised on magnetic nanoparticles, and (C) gum arabic.

### C. Removal of MB Dye

The produced MNPs and GA-MNPs were tested for their capacity to adsorb MB as a model compound from aqueous solutions by mixing 25 mg of fabricated nanoparticles with 50 mL of methylene blue ( $40 \text{ mg L}^{-1}$ ) in a test tube at 300 K. After adsorption, the magnetic nanoparticles were separated from the medium by applying a magnetic field. It was found that adsorption of MB reached equilibrium within 5 minutes, showing fast separation of MB from aqueous solution. The external surface adsorption allows MB access to the active sites resulting in fast equilibrium. Figure 8 shows that MB was removed efficiently when using GA-MNPs compared with naked MNPs, which means coating MNPs with GA enhanced the adsorption capability.



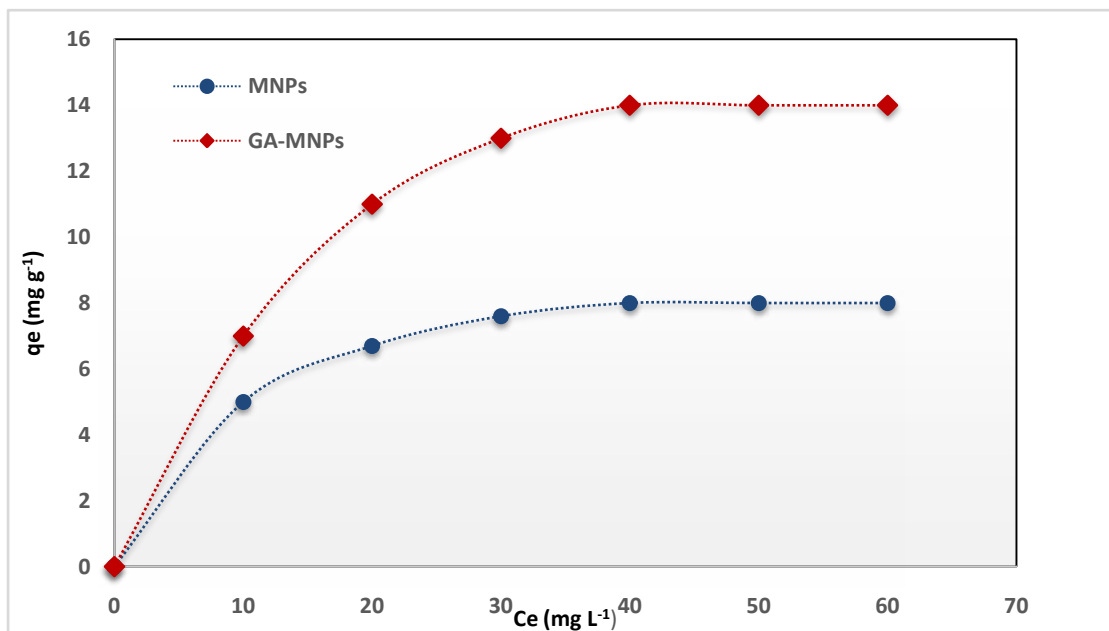


Fig. 8 Equilibrium isotherms for the adsorption of MB by MNPs, and GA-MNPs, adsorbent dose = 25 mg, MB concentration = 40 mg L<sup>-1</sup>, stirring speed = 350 rpm, temperature = 300 K.

The amount of dye adsorbed can be determined as a function of the concentration at a constant temperature that can be explained by adsorption isotherms. In this study, Langmuir isotherm was used to explain dye-ferrite interaction. The Langmuir isotherm is based on the physical hypothesis that assumes the monolayer adsorption is formed on a homogeneous surface of an adsorbent with no lateral interaction between adsorbed molecules, and that the adsorption energy is distributed homogeneously over the entire coverage surface [23]. The linear form of the Langmuir isotherm can be represented as follows:

$$\frac{C_{eq}}{q_e} = \frac{1}{b} \cdot C_{eq} + \frac{1}{Kb} [24]$$

Where  $C_{eq}$  is the concentration of solute remaining in solution at equilibrium (mg L<sup>-1</sup>),  $q_e$  is the amount of solute adsorbed per unit weight of adsorbent (mg g<sup>-1</sup>),  $b$  is the maximum adsorption capacity of sorbent corresponding to complete monolayer coverage (mg mg<sup>-1</sup>)  $K$ , is a Langmuir adsorption constant related to the energy of the adsorption (L mg<sup>-1</sup>). A plot of  $\frac{C_{eq}}{q_e}$  versus  $C_{eq}$  yields a straight line with slope  $\frac{1}{b}$  and intercept  $\frac{1}{Kb}$ . The Langmuir plot for the system studied is presented in Figure 9 that shows the equilibrium isotherms for the adsorption of MB by MNPs and GA-MNPs. The  $R^2$  values showed that the Langmuir model fit since the correlation coefficients of Langmuir isotherm were 0.9917 and 0.9947 for naked MNPs and GA-MNPs respectively. The maximum adsorption capacities were found to be 8.77 mg mg<sup>-1</sup> and 14.3 mg mg<sup>-1</sup> for MNPs and GA-MNPs respectively, and the values For MNPs and GA-MNPs were calculated as 0.5202 and 0.7527 L mg<sup>-1</sup>.

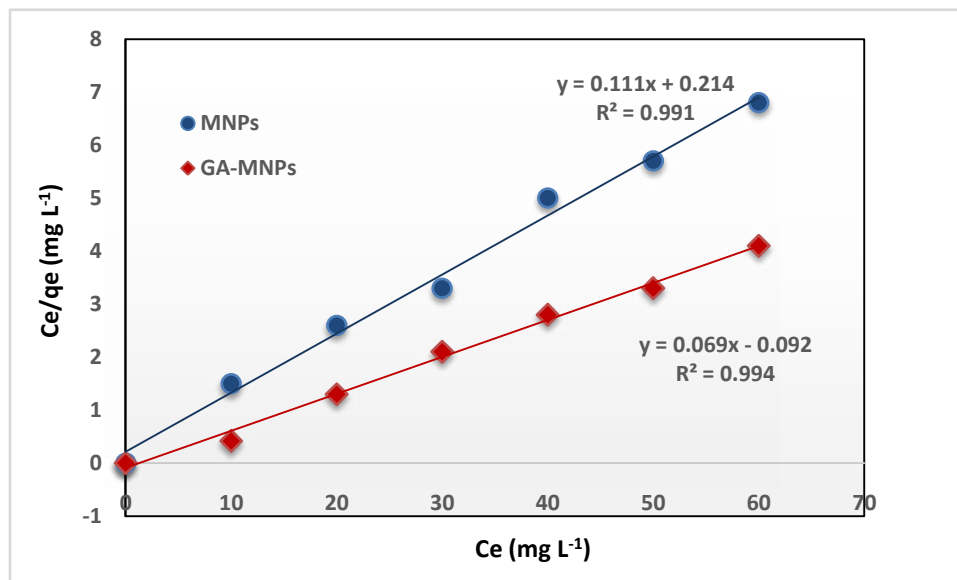


Fig. 9 linearized Langmuir isotherm for MB by MNPs and GA-MNPs.

The fundamental characteristics of the Langmuir equation can be presented in terms of dimensionless constant called equilibrium parameter ( $R_L$ ), which represents the essential features of the Langmuir isotherm and predicts its applicability. It can be defined by the following equation:

$$R_L = \frac{1}{1 + b C_o}$$

Where  $b$  is the Langmuir constant, and  $C_o$  is the initial concentration of MB dye.  $R_L$  values within the range  $0 < R_L < 1$  present favourable adsorption. In this study, values of  $R_L$  were found to be less than 1.0, as shown in Table 2, and approved that prepared MNPs and GA-MNPs are favourable for adsorption of MB, and also confirms the applicability of the Langmuir adsorption isotherm model.

Table 2 Separation factor  $R_L$  at different MB concentration.

Concentration	10	20	30	40	50	60
$R_L$ (MNPs)	0.1612	0.0876	0.0602	0.0458	0.0370	0.0310
$R_L$ (GA-MNPs)	0.1172	0.0622	0.0424	0.0321	0.0258	0.0221

The effect of temperature on the adsorption of MB by naked MNPs and GA-MNPs was studied using different temperatures (300 - 330 K), as can be seen in Figure 10. From the figure, it was found that by increasing the temperature, the adsorption capacities for MNPs and GA-MNPs increased indicating that both adsorption processes are endothermic, and maximum adsorption capacity was found to be  $14 \text{ mg g}^{-1}$ ,  $19 \text{ mg g}^{-1}$ ,  $25 \text{ mg g}^{-1}$ , and  $29 \text{ mg g}^{-1}$  at 300 K, 310 K, 320 K, and 330 K, respectively, while for GA-MNPs maximum adsorption capacity was found to be  $8 \text{ mg g}^{-1}$ ,  $12 \text{ mg g}^{-1}$ ,  $16 \text{ mg g}^{-1}$ , and  $21 \text{ mg g}^{-1}$  at 300 K, 310 K, 320 K, and 330 K, respectively. Moreover, the stability of GA on the surface of MNPs at high temperature (330K) was also investigated by collecting GA-MNPs in distilled water after the experiment and studying them using FT-IR spectroscopy. It was found that the heat treatment did not affect the GA coated the MNPs, which means the GA-MNPs was stable at high temperature.

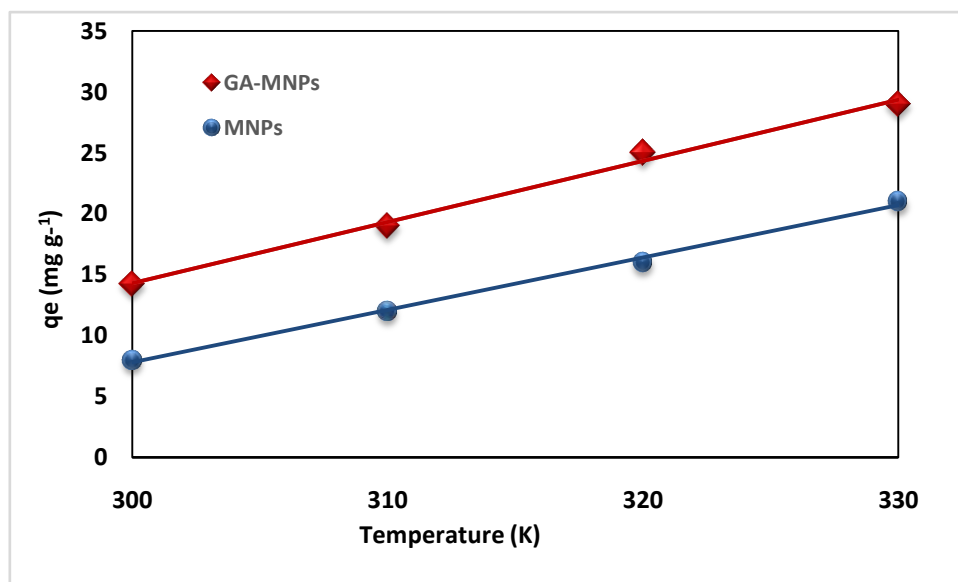


Fig. 10 Effects of temperature on the adsorption of MB by MNPs and GA-MNPs.

#### IV. CONCLUSION

In this study, magnetic nanoparticles were coated with GA and characterised by BET, TEM, SEM, EDAX, XRD, and FT-IR. Determination of the effectiveness of MB adsorption from aqueous solution on fabricated MNPs and GA-MNPs was investigated. Results indicated that the GA-coated magnetic nanoparticles showed high efficiency in removing MB in aqueous solution and the adsorption isotherm of GA at the surface of bare magnetite followed a Langmuir model. The removal efficiency increased with increasing temperature, which means the adsorption process is endothermic in nature. The results of this study open the possibility for using GA-MNPs in applications involving the removal of dyes from aqueous solution and for waste-water treatment.

#### REFERENCES

- [1] Guo, J.-Z., et al., *Removal of methylene blue from aqueous solutions by chemically modified bamboo*. Chemosphere, 2014. **111**: p. 225-231.
- [2] Bhattacharyya, K.G. and A. Sharma, *Kinetics and thermodynamics of Methylene Blue adsorption on Neem (Azadirachta indica) leaf powder*. Dyes and Pigments, 2005. **65**(1): p. 51-59.
- [3] Sun, S. and H. Zeng, *Size-Controlled Synthesis of Magnetite Nanoparticles*. Journal of the American Chemical Society, 2002. **124**(28): p. 8204-8205.
- [4] Wang, N., et al., *Adsorption of environmental pollutants using magnetic hybrid nanoparticles modified with  $\beta$ -cyclodextrin*. Applied Surface Science, 2014. **305**: p. 267-273.
- [5] Gordani, G.R., A. Ghasemi, and A. Saïdi, *Enhanced magnetic properties of substituted Sr-hexaferrite nanoparticles synthesized by co-precipitation method*. Ceramics International, 2014. **40**(3): p. 4945-4952.
- [6] Bolto, B.A., *Magnetic particle technology for wastewater treatment*. Waste Management, 1990. **10**(1): p. 11-21.
- [7] Fuertes, A.B. and P. Tartaj, *A Facile Route for the Preparation of Superparamagnetic Porous Carbons*. Chemistry of Materials, 2006. **18**(6): p. 1675-1679.
- [8] Yang, N., et al., *Synthesis and properties of magnetic Fe<sub>3</sub>O<sub>4</sub>-activated carbon nanocomposite particles for dye removal*. Materials Letters, 2008. **62**(4-5): p. 645-647.
- [9] Kentish, S.E. and G.W. Stevens, *Innovations in separations technology for the recycling and re-use of liquid waste streams*. Chemical Engineering Journal, 2001. **84**(2): p. 149-159.
- [10] Mao, P., et al., *Phase separation induced molecular fractionation of gum arabic—Sugar beet pectin systems*. Carbohydrate Polymers, 2013. **98**(1): p. 699-705.
- [11] Abuarra, A., et al., *Fabrication and characterization of gum Arabic bonded Rhizophora spp. particleboards*. Materials & Design, 2014. **60**: p. 108-115.
- [12] Ali, A., et al., *Effect of gum arabic as an edible coating on antioxidant capacity of tomato (Solanum lycopersicum L.) fruit during storage*. Postharvest Biology and Technology, 2013. **76**: p. 119-124.

# International Journal of Innovative Research in Science, Engineering and Technology

(An ISO 3297: 2007 Certified Organization)

Vol. 3, Issue 8, August 2014

- [13] Kong, H., et al., *Synthesis and antioxidant properties of gum arabic-stabilized selenium nanoparticles*. International Journal of Biological Macromolecules, 2014. **65**: p. 155-162.
- [14] Roque, A.C.A., et al., *Biocompatible and bioactive gum Arabic coated iron oxide magnetic nanoparticles*. Journal of Biotechnology, 2009. **144**(4): p. 313-320.
- [15] Nishi, K. and A. Jayakrishnan, *Self-gelling primaquine-gum arabic conjugate: an injectable controlled delivery system for primaquine*. Biomacromolecules, 2007. **8**(1): p. 84-90.
- [16] Lambert, J., F. Weinbreck, and M. Kleerebezem, *In Vitro Analysis of Protection of the Enzyme Bile Salt Hydrolase against Enteric Conditions by Whey Protein– Gum Arabic Microencapsulation*. Journal of agricultural and food chemistry, 2008. **56**(18): p. 8360-8364.
- [17] Chockalingam, A.M., et al., *Gum arabic modified Fe<sub>3</sub>O<sub>4</sub> nanoparticles cross linked with collagen for isolation of bacteria*. Journal of nanobiotechnology, 2010. **8**(1): p. 30-39.
- [18] Tan, K.A., et al., *Removal of Cationic Dye by Magnetic Nanoparticle (Fe<sub>3</sub>O<sub>4</sub>) Impregnated onto Activated Maize Cob Powder and Kinetic Study of Dye Waste Adsorption*. APCBEE Procedia, 2012. **1**: p. 83-89.
- [19] Loekitowati Hariani, P., et al., *Synthesis and Properties of Fe<sub>3</sub>O<sub>4</sub> Nanoparticles by Co-precipitation Method to Removal Procion Dye*. International Journal of Environmental Science and Development, 2013. **4**(3): p. 336-340.
- [20] Enriquez, P.M., et al., *Delivery of therapeutic agents to receptors using polysaccharides*. 1996, Google Patents.
- [21] Li, Y., et al., *Rapid screening and identification of  $\alpha$ -amylase inhibitors from *Garcinia xanthochymus* using enzyme-immobilized magnetic nanoparticles coupled with HPLC and MS*. Journal of Chromatography B, 2014. **960**: p. 166-173.
- [22] Banerjee, S.S. and D.-H. Chen, *Fast removal of copper ions by gum arabic modified magnetic nano-adsorbent*. Journal of Hazardous Materials, 2007. **147**(3): p. 792-799.
- [23] Hu, J., G. Chen, and I.M. Lo, *Selective removal of heavy metals from industrial wastewater using maghemite nanoparticle: performance and mechanisms*. Journal of environmental engineering, 2006. **132**(7): p. 709-715.
- [24] Salima, A., et al., *Application of *Ulva lactuca* and *Systoceira stricta* algae-based activated carbons to hazardous cationic dyes removal from industrial effluents*. Water Research, 2013. **47**(10): p. 3375-3388.